Near-Infrared Resonance Raman Spectroscopy of the Special Pair and the Accessory Bacteriochlorophylls in Photosynthetic Reaction Centers

Nerine J. Cherepy,† Andrew P. Shreve,† Laura J. Moore,‡ Stefan Franzen,‡ Steven G. Boxer,*,‡ and Richard A. Mathies*,†

Department of Chemistry, University of California, Berkeley, California 94720, and Department of Chemistry, Stanford University, Stanford, California 94305

Received: December 14, 1993; In Final Form: April 5, 1994®

Rapid-flow resonance Raman spectra of the primary electron donor (a bacteriochlorophyll dimer known as P) and of the monomeric accessory bacteriochlorophylls (B) in the bacterial photosynthetic reaction center of *Rb. sphaeroides* have been obtained at 5 °C. The spectra were obtained using a shifted excitation Raman difference technique with excitation at 850 nm for the P spectrum and 800 nm for the B spectrum. Raman bands at 187, 204, 332, 564, 684, 730, 899, and 1163 cm^{-1} are found in common in the P and B spectra, while unique modes appear in the low-frequency region of the special pair at 34, 71, 95, 128, and 484 cm^{-1}. The remaining strongly Raman-active monomer modes at 353, 385, 621, 761, 1010, 1114, and 1132 cm^{-1} were not detected in the dimer spectrum. No substantial resonance Raman activity is observed above 1200 cm^{-1} for either chromophore, indicating that high-frequency modes are not strongly coupled to the optical excitation in the Q_y absorptions of B or P. The Raman spectrum shows that the electronic excitation of P is coupled to at least 14 vibrational degrees of freedom, including low-frequency modes at 34, 71, 95, and 128 cm^{-1}. The Raman scattering cross sections for the modes of B are approximately an order of magnitude larger than those for analogous modes of P. This difference suggests that the excited electronic state of P is damped by rapid vibronic relaxation processes that are not present in B. The complete analysis of these resonance Raman results will lead to the development of specific multimode models for the excited-state structural dynamics and relaxation of the chromophores in reaction centers.

Introduction

The photosynthetic reaction center (RC)[1] is a pigment-protein complex that mediates a highly efficient light-driven electron-transfer reaction (for recent reviews see refs 2–5). In the bacterial reaction center of *Rb. sphaeroides*, charge separation from the lowest-energy excited singlet state of a strongly interacting pair of bacteriochlorophyll$_a$ ($Bchl_a$) molecules, called the special pair (P), to a bacteriopheophytin occurs within 3 ps at room temperature. To understand the rapid and efficient photochemistry of RCs, a complete description of the excited-state properties of the primary electron donor, P, and of the other pigments in this complex is needed.

The lowest-energy, near-infrared absorption bands of the RC result from the Q_y electronic transitions of the special pair, two monomeric Bchl molecules (B), and two bacteriopheophytin molecules. For RCs isolated from *Rb. sphaeroides*, the near-infrared absorption spectrum at room temperature contains three distinct peaks at about 860, 800, and 760 nm. The 860-nm transition, due to P, is assigned to the lower-energy member of a pair of excitonic dimer states. The absorption feature at 800 nm is due to the two monomeric Bchl molecules, although weak absorption of the upper excitonic state of P might also contribute.[6–8] The 760-nm transition is mostly due to the bacteriopheophytins.

A number of techniques have been used to study the excited-state relaxation rates and geometry changes of B and P. Low-temperature hole-burning spectroscopy produces a relatively small, sharp feature in the P absorption band, accompanied by a strong, broad sideband,[9–13] suggesting that the absorption spectrum of P is broadened by unresolved vibrational progressions, including those from highly-displaced low-frequency modes. In contrast, the Q_y transitions of monomeric Bchl, chlorophyll in solution, and presumably B in the RC are characterized by small ground-to-excited-state nuclear displacements.[14] Stark spectroscopy has revealed that the excited state of P has both a large permanent dipole (about 3 times that of monomeric Bchl) and a large polarizability.[15–18] The excited state of B is neither very dipolar nor polarizable, in agreement with the excited-state properties of monomeric Bchl in glasses.[16,17] Both the large nuclear displacements and the big change in electrostatic properties upon excitation are consistent with the presence of charge-transfer character in the excited state of P.[5,19] In addition to these experiments, time-resolved spectroscopy has established that excitation of P leads to charge separation on the picosecond time scale,[20–25] while excitation of B leads to an ultrafast (≈100 fs) energy transfer from the excited state of B to the excited state of P.[21,25]

Resonance Raman vibrational spectroscopy and Raman intensity analysis are powerful methods for obtaining multimode information about excited-state structure and dynamics.[26–30] The modes that appear in a resonance Raman spectrum are those that are coupled to the resonant electronic transition, and the intensity of the Raman scattering reflects both the strength of this coupling and the dynamics that occur in the excited electronic state. A self-consistent modeling of the absorption spectrum and the excitation-wavelength-dependent resonance Raman cross sections for RCs could be used to develop a multidimensional excited-state potential energy surface and a description of the electronic-state relaxation rates, as has been demonstrated for other photobiological systems.[26,28]

In an earlier report, we demonstrated that shifted excitation Raman difference spectroscopy can be used to obtain resonance Raman spectra of RCs using resonant near-infrared excitation, even in the presence of the background fluorescence.[31,32] Here, we present more complete and higher signal-to-noise resonance Raman spectra obtained using excitation on resonance with the Q_y transitions of both B and P. Comparison of the Raman spectra of B and P reveals differences in the modes that are coupled to

† University of California.
‡ Stanford University.
* Authors to whom correspondence should be addressed.
® Abstract published in *Advance ACS Abstracts*, May 15, 1994.

0022-3654/94/2098-6023$04.50/0

their electronic excitations. We have also quantified the scattering strength at each excitation wavelength by using an internal scattering standard. The intensity of the Raman scattering from P is much weaker than that from B, reflecting differences in excited-state structural relaxation or dephasing in these two chromophores. These results provide new information for understanding the unique properties of the special pair, and they provide multimode information that will aid in the interpretation of other vibronic spectroscopies such as hole burning or the oscillations that have recently been reported in femtosecond time-resolved absorption spectra of RCs.[24,33]

Experimental Section

Q_A-containing RCs were isolated from the R-26 mutant of *Rb. sphaeroides* as described previously.[34,35] They were suspended in buffered detergent solution (0.025% LDAO, 10 mM TRIS, pH 8) or in a 1/1 (v/v) mixture of buffered detergent and ethylene glycol.

Ethylene glycol was used as an internal Raman intensity standard. Raman scattering from the 864-cm^{-1} mode of ethylene glycol can be observed when the RC concentration is reduced enough to compensate for the resonance enhancement of the RC scattering. For quantitative work, the intensity of the strong 730-cm^{-1} RC mode was obtained relative to that of the 864-cm^{-1} ethylene glycol mode using a low concentration solution of RCs ($OD_{800} \approx 0.07$/cm for 800-nm excitation and $OD_{800} \approx 0.7$/cm for 850-nm excitation) where the two modes have nearly equal intensity. The full spectra were then obtained separately using more concentrated solutions (OD $\approx$ 3.0/cm at the excitation wavelength) without ethylene glycol. Excitation powers (at 850 nm) were typically 5 mW for measuring the full spectrum and 2 mW for measuring the relative intensities with the 50% ethylene glycol solution.

The laser excitation and collection of scattered light were performed as described previously,[31] except for the use of a cylindrical rather than a spherical lens to focus the incident laser beam on a rapidly flowing solution of RCs. Raman spectra were recorded with a cryogenically-cooled CCD detector (LN/CCD-1152, Princeton Instruments) coupled to a subtractive-dispersion, double spectrograph[36] equipped with one 600 groove/mm grating and one 1200 groove/mm grating, both blazed at 750 nm (10-cm^{-1} entrance slit). All spectra were corrected for the wavelength dependence of the detection efficiency by use of a standard lamp. The enhanced signal-to-noise in comparison with our previous results[31] is due mostly to the change to a cylindrical focusing geometry, which increases the excitation (and scattering) volume for a fixed photoalteration parameter.[37] Furthermore, significant noise in excess of the shot-noise limit in the 1000–1300-cm^{-1} region for 850-nm excitation has been eliminated by attaching a N_2 purge to the spectrograph to eliminate water absorption interference.[38]

The experimental conditions used to obtain the rapid-flow spectrum of P were chosen to minimize photoalteration effects. Spectra were obtained with a cylindrically focused beam illuminating an area of approximately 5×10^{-4} cm^2 (1 mm × 50 μm). Assuming a rectangular beam profile, the average fraction of molecules in the illuminated volume, f, that have absorbed a photon that leads to photochemistry is given by

$$f = 1 - (1/F)(1 - e^{-F}) \quad (1)$$

where F, the photoalteration parameter, is the probability that any single RC was excited after passage through the beam.[37] Here $F = 2303\epsilon\Phi P/(N_A a v)$, where ϵ is the molar extinction coefficient (ϵ = 110 000 at 850 nm), Φ is the photochemical quantum yield, a is the beam dimension perpendicular to the flow direction, v is the linear flow velocity, and N_A is Avogadro's number. Since this equation assumes that the bleaching recovery is slow compared to the transit time through the beam, an assumption that may not be valid for RCs, this calculation will, if anything, overestimate the effect of bleaching on the resonance Raman spectrum. Assuming a quantum yield of unity and using a flow velocity of 200 cm/s, we calculate that f = 0.20 for the 5-mW full spectra and 0.09 for the 2-mW spectra. In addition, the value of f was determined empirically from a fit of eq 1 to both the Raman and fluorescence saturation data. Raman and RC fluorescence intensities were measured with incident laser powers ranging from 0.20 to 19 mW. The best fit to eq 1 for both sets of data yielded $F = 0.15P$, where P is in milliwatts. This analysis gives f = 0.29 at 5 mW and f = 0.14 at 2 mW, in good agreement with the calculated values considering the simplicity of the model and the uncertainty of the input parameters. Powers of 2 mW (f = 0.14) were used in the determination of the relative scattering cross sections, producing a $\approx$7% decrease of the RC scattering intensity due to photochemical bleaching.[37] To obtain full spectra with high signal-to-noise, 5-mW excitation power at 850 nm was used, leading to a 20% decrease in the observed signal. This bleaching will not affect the determination of the full spectrum unless a photochemical product exhibits significant Raman scattering. Two observations indicate that this is unlikely. First, time-resolved absorption studies show that once P^+ is formed there is no appreciable absorption in the 820–900-nm region. Second, experiments in both the low-frequency and mid-frequency region reveal no detectable signal for 850-nm excitation when P is chemically oxidized to P^+.[31]

As in our previous work,[31,32] we found it advantageous to use a shifted excitation Raman difference technique to identify RC Raman bands in the presence of the intrinsic fluorescence background ($\Phi_f \approx 4 \times 10^{-4}$).[41] In this technique, two emission spectra are obtained with the excitation laser frequency shifted by 10 cm^{-1} relative to one another, but with all other experimental conditions identical. These spectra are then subtracted to yield a shifted excitation Raman difference spectrum. In all reported spectra, the difference spectrum is the shifted minus the unshifted excitation spectrum, and the x axis corresponds to the spectral axis for the unshifted excitation frequency. Derivative-like features, corresponding to Raman lines, are then fit to a model which assumes that the Raman spectrum is a difference of Gaussian peaks. The amplitude, position, and width of each peak are determined in a nonlinear least-squares fit, and these parameters are then used to generate the Gaussian peaks shown in the simulated Raman spectrum. Our previous work has demonstrated the accuracy of this method, by presenting directly detected spectra (acquired with extended accumulation times) that match spectra simulated from the difference spectra.[31,32]

Results

The resonance Raman spectra obtained with excitation at 800 nm (resonant with B) and with excitation at 850 nm (resonant with P) are shown in Figures 1 and 2, respectively. The comparison of the 730-cm^{-1} RC mode and the 864-cm^{-1} ethylene glycol standard mode is presented for 800- and 850-nm excitation in Figure 3, A and B, respectively. Three key results are evident. First, a comparison of Figures 1 and 2 demonstrates that the spectra excited resonantly with B and P are qualitatively different, displaying significantly different modes and intensity patterns. Table 1 lists experimental mode frequencies and relative intensities. In particular, the 30–150-cm^{-1} regions of the spectra are very different, with four strong modes present in the P spectrum and none in the B spectrum. All the Raman lines reported previously[31] are observed, along with a few smaller peaks that can now be identified with the improved signal-to-noise. Relatively weak P modes at 484, 564, 585, and 1163 cm^{-1} can now be resolved, and a full B spectrum is presented for the first time.

The second result is that resonance Raman scattering from the monomers (800-nm excitation) is significantly stronger than that from the special pair (850-nm excitation). For example, the absolute intensity of the 730-cm^{-1} mode with 800-nm excitation is approximately 10 times larger than the 730-cm^{-1} mode with

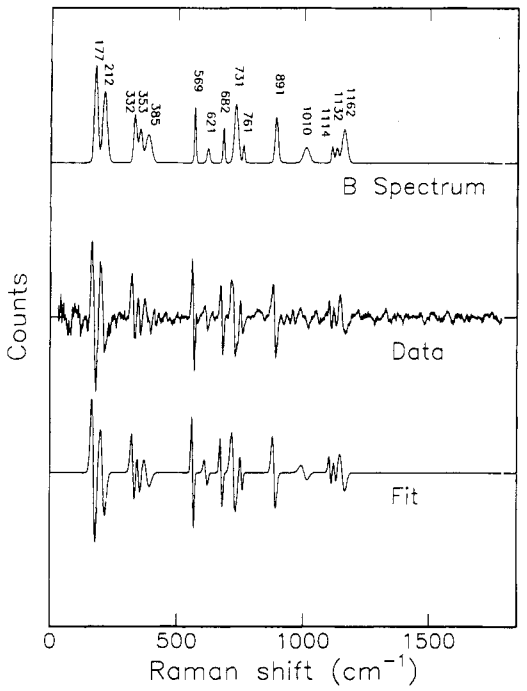

Figure 1. Shifted excitation Raman difference spectrum of B using 800-nm excitation (T = 278 K, P = 5 mW). The middle trace shows the intensity-corrected Raman difference data, the bottom trace is the fit to the difference data, and the top trace is the spectrum generated from the fit. Some structure in the high-frequency region is reproducible but too weak to be fit reliably.

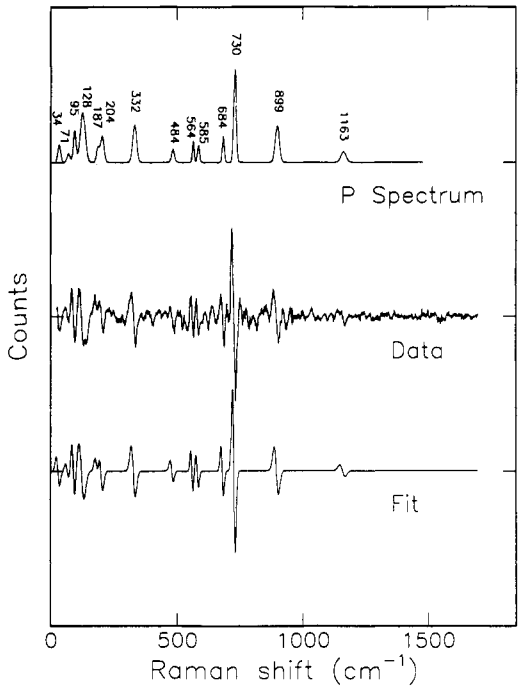

Figure 2. Shifted excitation Raman difference spectrum of P using 850-nm excitation (T = 278 K, P = 5 mW). The middle trace shows the intensity-corrected Raman difference data, the bottom trace is the fit to the difference data, and the top trace is the spectrum generated from the fit.

850-nm excitation. This result is evident from the data shown in Figure 3, where comparable intensities of the 730-cm^{-1} RC mode relative to the ethylene glycol mode are obtained using a 7.8 times more concentrated sample for excitation in P than for excitation in B. Independent experiments on several different samples were averaged, giving a ratio of the cross section of the 730-cm^{-1} mode to the ethylene glycol mode of (17 ± 6) × 10^6 at 800 nm and (2.2 ± 0.6) × 10^6 at 850 nm. Accounting for the wavelength dependence of the ethylene glycol cross section, the 730-cm^{-1} mode is about 10 times stronger in B than in P.

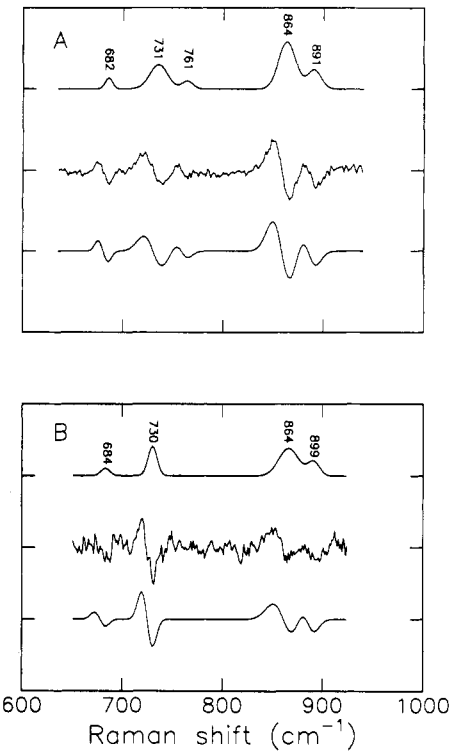

Figure 3. Mid-frequency Raman spectra of RCs in a 50% v/v mixture of buffer and ethylene glycol. For each panel, the middle trace shows the Raman difference data, the bottom trace is the fit to the difference data, and the top trace is the spectrum generated from the fit. The ethylene glycol peak is observed at 864 cm^{-1} in both panels. (A) Spectrum of B obtained with 2.5 mW at 800 nm. The sample absorbance at 800 nm is 0.072/cm. The ratio of peak areas for the RC mode near 730 cm^{-1} and the ethylene glycol is 0.53, and the relative cross section is 21 × 10^6. (B) Spectrum of P obtained with 1.4 mW at 850-nm excitation. The sample absorbance at 800 nm is 0.56/cm (7.8 times that used in (A)). The ratio of peak areas for the RC mode near 730 cm^{-1} and the ethylene glycol mode is 0.48, and the relative cross section is 2.7 × 10^6. For these data, after correction for the difference in concentrations and the wavelength dependence of the ethylene glycol cross section, the cross section of the 730-cm^{-1} mode is 10 times stronger for excitation at 800 nm than for excitation at 850 nm.

TABLE 1: Frequencies and Intensities of Resonance Raman Bands of P and B

P		B	
ν, cm^{-1}	intensity[a]	ν, cm^{-1}	intensity[a]
34	0.22		
71	0.12		
95	0.36		
128	1.05		
187	0.17	177	1.43
204	0.38	212	1.35
332	0.61	332	0.64
		353	0.48
		385	0.71
484	0.16		
564	0.16	569	0.40
585	0.16		
		621	0.17
684	0.23	682	0.27
730	1.0	731	1.0
		761	0.14
899	0.63	891	0.61
		1010	0.40
		1114	0.15
		1132	0.17
1163	0.23	1162	0.72

[a] Intensities are relative to the 730-cm^{-1} mode.

A third important observation is the lack of intense modes in the 1200–1700-cm^{-1} region with excitation resonant with the Q_y transitions of both B and P (Figures 1 and 2). It has been suggested that this observation is due to the low efficiency of front-

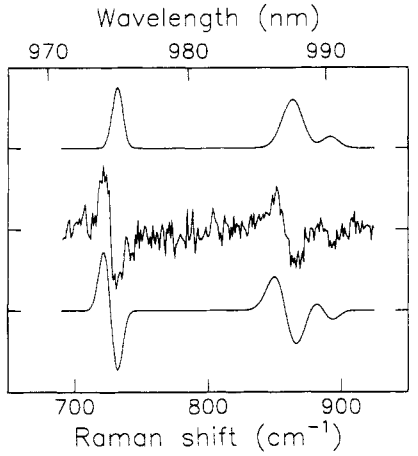

Figure 4. Mid-frequency Raman spectrum of RCs obtained using 910-nm excitation. The sample absorbance (1-cm path length) at the excitation wavelength is 0.2 in a 50% v/v mixture of buffer and ethylene glycol. The top axis shows the absolute wavelength of the detected signal. For comparison with Figure 1, 990-nm emission corresponds to a Raman shift of 1664 cm^{-1} from 850 nm.

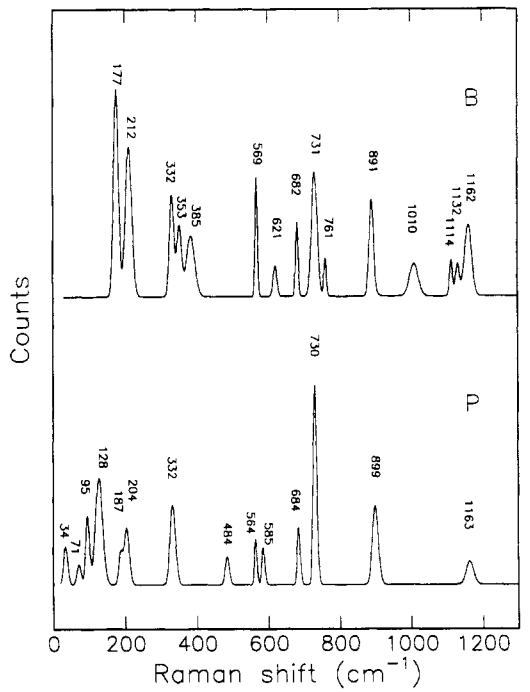

Figure 5. Comparison of the P and B resonance Raman spectra obtained using shifted excitation Raman difference spectroscopy.

illuminated CCD detectors at wavelengths approaching 1000 nm.[42] However, the detection response for our system at 993 nm, the longest wavelength detected here, is still about 10% of the maximum detection sensitivity, and *all reported spectra have been sensitivity corrected.* To amplify this point further, Figure 4 presents a spectrum taken with excitation at 910 nm. The 730-cm^{-1} RC line and the 864-cm^{-1} ethylene glycol line are clearly detected, and even the weaker RC mode at 899 cm^{-1} is apparent. The detection window is centered at ≈980 nm (10 200 cm^{-1}), which corresponds to a window centered 1580 cm^{-1} to the red of 850 nm. This demonstrates that the Raman spectra shown in Figures 1 and 2 were acquired with a system that is capable of detecting any strong modes of frequencies less than 1700 cm^{-1} that might be enhanced with either 800- or 850-nm excitation. As in our previous work, the simple observation is that for Q_y resonance excitation B and P do not exhibit strong scattering in modes higher than 1200 cm^{-1}.

Discussion

Resonance Raman spectroscopy probes both nuclear and electronic dynamics associated with the resonantly excited transition.[43-46] Vibrational frequencies observed in a resonance Raman spectrum are the ground-state frequencies of nuclear motions that are coupled to the resonant electronic transition. Thus, modes observed in the resonance Raman spectrum give direct information about the nuclear coordinates along which the molecule distorts upon electronic excitation. Scattering cross sections give information on the magnitude of displacement of the modes in the excited electronic state as well as the electronic dephasing time. Quantitative analysis of the intensities of the Raman bands and mode assignments can provide a detailed picture of the nuclear distortions and relaxation occurring after electronic excitation.

We will begin our resonance Raman analysis of RCs by comparing the vibrational modes of B and P. Then these results are discussed in the context of previous spectroscopic studies of monomeric Bchl, B, and P. Finally, the relationship between excited-state dynamics and the resonance Raman cross sections of B and P is explored.

Resonance Raman Spectra of B and P. To facilitate comparison, the expanded spectra of B and P are presented in Figure 5. Since both B and P contain Bchl, initially one would expect that the monomer modes would also be observed in the dimer spectrum and that the enhancement pattern would be similar. However, given that the Raman cross sections in resonance with P are about an order of magnitude smaller than cross sections for the same modes in B, some weak monomer modes may be difficult to detect in the P spectrum. At the next level of analysis, differential resonance enhancement (or deenhancement) of certain monomer modes could arise in the dimer spectrum due to the unique properties of the dimer excited electronic state. Finally, formation of the dimer from two independent monomers results in six new vibrational degrees of freedom which involve changes in the distance and orientation of the two monomers. Comparison of the vibrational structure of B and P by spectral region reveals examples of each of these expectations.

Low-Frequency Region, 0–500 cm^{-1}. P exhibits modes at 34, 71, 95, 128, and 484 cm^{-1} that do not appear in the B spectrum. There is a possibility that some of these may be overtones or combination bands. For instance, the 71-cm^{-1} peak may be an overtone of the 34-cm^{-1} mode, or the 34-cm^{-1} peak could be a difference band of the 128- and 95-cm^{-1} modes. The B spectrum lacks any strong modes in this frequency range, although a feature appears near 128 cm^{-1} that is too weak to be fit reliably. An early semiempirical calculation predicted an intradimer mode at 100 cm^{-1} which may correspond to either the 95- or 128-cm^{-1} mode.[47] There are P modes at 187 and 204 cm^{-1} that appear to correspond to strong B modes at 177 and 212 cm^{-1}. A mode at 332 cm^{-1} is present in both the P and B spectra. Finally, some modes are observed in the B spectrum but are not strong enough to be fit in the P spectrum. The 353- and 385-cm^{-1} modes fall in this category.

Mid-Frequency Region, 500–1000 cm^{-1}. In this spectral range many modes are conserved between the monomer and the dimer. The P modes at 564 and 585 cm^{-1} appear to correspond to the single strong B mode at 569 cm^{-1}. The P modes at 684, 730, and 899 cm^{-1} correspond to the B modes at 682, 731, and 891 cm^{-1}. There are B modes at 621 and 761 cm^{-1} and some weak features at about 650, 920, 945, and 965 cm^{-1} not seen in the P spectrum. Mode assignments shown in Table 2 were proposed by Mattioli et al.[48] and Noguchi et al.[49] for Bchl. In this region, the modes are assigned as in-plane ring distortions.

High-Frequency Region, 1000–1800 cm^{-1}. Only a few weak high-frequency modes are observed with excitation in resonance with the Q_y transitions of P and B. This is markedly different from the strong high-frequency scattering observed with Soret band excitation of these chromophores.[50,51] A line appearing at 1162 cm^{-1} in B and at 1163 cm^{-1} in P is the only strong feature appearing in the P spectrum in this region. Modes at 1010, 1114, and 1132 cm^{-1} are seen only in the B spectrum. In addition to the reported modes, some very weak but reproducible features

TABLE 2: Comparison of Vibrational Frequencies for P and B[m]

P[a]	B[b]	Bchl[c]	Bchl[d]	Bchl[e]	Bchl[f]	Bchl[g]	Bchl[h]	Bchl[i]	RC[j]	RC[k]	assignnt[l]
187	177					164	166				
204	212					196	194				
332	332					342		340		335	
	385					380					
564	569	564	565	567	569	568		560	563	565	
	621					624			617		δCCC[c]
684	682		685			683			669		
730	731	730	730	728	730	729		750	727	728	δCNC, δC_mH[c]
	761					763					
899	891	892	894	897	898	897		920	893	894	δCNC[d]
	1010	1014	1010	1015	1020	1026			1013		νC_aC_b[c]
	1114	1118	1117	1116	1116	1113					νCN(δCNC)[c]
	1132	1137	1137	1142	1142	1135			1133		νCN(δCNC)[c]
1163	1162	1157	1159	1173	1176	1174					νCN[c]

[a] Resonance Raman spectrum of P, λ_{ex} = 850 nm, this work. [b] Resonance Raman spectrum of B, λ_{ex} = 800 nm, this work. [c] FT Raman spectrum of Bchl in tetrahydrofuran, λ_{ex} = 1064 nm.[48] [d] FT Raman spectrum of Bchl in a pyrazine film, λ_{ex} = 1064 nm.[49] [e] FT Raman spectrum of Bchl in chromatophores from *Rb. sphaeroides* antennae, λ_{ex} = 1064 nm.[49] [f] FT Raman spectrum of Bchl in chromatophore fragments of *Rsp. rubrum*, λ_{ex} = 1064 nm.[53] [g] Site selection emission spectra of Bchl in a TEA (triethylamine) film, λ_{ex} = 703.2 (0–1 vibronic region).[57] [h] Hole-burning spectrum of Bchl in TEA, λ_{ex} = 780 nm (near 0–0 transition).[58] [i] Hole-burning spectrum of B850 from the *Rb. sphaeroides* antennae, excited near 853 nm.[14] [j] FT Raman spectrum of RCs, λ_{ex} = 1064 nm.[52] [k] FT Raman spectrum of RCs, λ_{ex} = 1064 nm.[54,53] [l] δ = in-plane deformation, ν = stretch. [m] Some of these spectra contain additional modes, mostly weaker, which were not observed using resonance Raman spectroscopy.

may be discerned in the B spectrum, at about 1230, 1270, 1300, 1345, 1395, 1460, and 1650 cm^{-1}, but they are too small to be fit reliably. The modes in this spectral region have been assigned as predominately C–C and C–N stretching motions.[48]

Comparison with Other Spectral Studies. Our resonance Raman spectra of B and P can be compared with other vibrationally-resolved spectra of $Bchl_a$-containing species obtained using the techniques of preresonant Fourier transform (FT) Raman spectroscopy, site-selective emission spectroscopy, and hole burning. Table 2 summarizes this comparison. Our goal here is to understand which vibrational modes are characteristically coupled to the Q_y transition of $Bchl_a$-containing species and how the results of these different techniques compare to the resonance Raman spectra.

FT Raman spectra have been taken of $Bchl_a$-containing systems with 1064-nm excitation, which is preresonant to all Bchl electronic states. FT Raman spectra of both Bchl monomers and RCs have been reported, and they provide a consistent set of $Bchl_a$ modes. The spectrum of $Bchl_a$ in a pyrazine film[49] contains modes at 565, 685, 730, 894, 1010, 1117, 1137, and 1159 cm^{-1}. These frequencies correspond to the strong modes in our resonance Raman spectrum of B at 569, 682, 731, 891, 1010, 1114, 1132, and 1162 cm^{-1}. Noguchi et al. also report a spectrum of chromatophores from a light harvesting complex of *Rb. sphaeroides*, exhibiting strong modes at 567, 728, 897, 1015, 1116, 1142, and 1173 cm^{-1}. An FT Raman spectrum of $Bchl_a$ in tetrahydrofuran similarly exhibits modes at 564, 730, 892, 1014, 1118, 1137, and 1157 cm^{-1}.[48] A 1064-nm FT Raman spectrum of RCs (uncorrected for the possible bleaching of P)[52] contains strong modes at 563, 617, 669, 727, 893, 1013, and 1113 cm^{-1} which may be preresonant B modes (or possibly resonant P^+ modes).[53] These comparisons establish that the modes found in our B spectrum are all typical of $Bchl_a$-containing species.

An FT Raman spectrum of P was obtained by subtracting a spectrum of chemically oxidized RCs from a spectrum of functioning RCs.[54] The FT Raman spectrum did not extend to low frequencies, but the middle frequency region of this spectrum shows prominent modes at 728 and 894 cm^{-1}, in good agreement with modes we observe at 730 and 899 cm^{-1}. In all the FT Raman experiments on Bchl systems, some weaker higher frequency modes are also observed. The large relative enhancement of the high-frequency modes in the FT Raman spectra compared to resonance Raman spectra could result either from higher electronic state contributions to the preresonant FT Raman scattering or from differences in intensity patterns between resonance and preresonance excitation.[55]

In addition to FT Raman studies, a previous report of the low-frequency resonance Raman spectrum has also been made.[56] The 95- and 128-cm^{-1} modes we observe are likely to be the same modes reported in this experiment at 102 and 138 cm^{-1}. Another recently published resonance Raman study of RCs[42] is discussed further below.

Other spectroscopic techniques have been used to provide vibrational information about $Bchl_a$-containing species. A site-selective fluorescence spectrum of $Bchl_a$ in a triethylamine glass[57] has been analyzed to reveal intensities and ground- and excited-state frequencies of modes coupled to the Q_y transition. The ground-state frequencies of the 13 strongest modes observed for Bchl are 164, 196, 342, 568, 624, 683, 729, 897, 950, 1026, 1113, 1135, and 1174 cm^{-1}. All these lines can be identified with lines in our spectrum of B. Furthermore, all the B modes we observe are observed in the fluorescence data.[57] Also, nonphotochemical hole-burning spectra of $Bchl_a$ in a triethylamine glass[58] and of B850 from the B800–850 light-harvesting complex of *Rb. sphaeroides*[14] contain a sharp, intense feature accompanied by small sidebands, revealing vibronic coupling to some of the same modes as those observed in the resonance Raman spectrum of B. In the nonphotochemical hole-burning spectrum of $Bchl_a$, modes are reported at 166 and 194 cm^{-1}.[58] These excited electronic state frequencies appear to correspond to modes we observe in the Raman spectrum of B with ground electronic state vibrational frequencies at 177 and 212 cm^{-1}. The hole-burning spectrum of B850 includes structure at 340, 560, 750, and 920 cm^{-1},[14] apparently corresponding to the strong B Raman modes at 332, 569, 730, and 891 cm^{-1}. Some vibronic structure has also been reported in photochemical hole-burning experiments on the P band of *Rb. sphaeroides* RCs. The hole consists of a weak, narrow feature, accompanied by a broad, intense phonon sideband. In the phonon sideband, a weak resolved feature is observed at ≈120 cm^{-1},[13,59] corresponding in frequency to the strong mode in the resonance Raman spectrum of P at 128 cm^{-1}.

To summarize, many investigators, using different techniques, have characterized the vibrational frequencies and the relative intensities of modes coupled to the Q_y transition of $Bchl_a$ and monomers of $Bchl_a$ bound to proteins. There is good agreement in mode frequencies and relative intensities among all the spectra of monomeric $Bchl_a$, including the resonance Raman spectrum of B reported here. In addition, the resonance Raman spectrum of P reported here is seen to contain a subset of these $Bchl_a$ monomer modes and to compare favorably with the FT Raman spectrum of P in the region where these data overlap.

Resonance Raman spectra of B and P have also been presented by Palaniappan et al.[42] In spectra taken with several excitation

wavelengths through the B and P absorption bands, ≈20 modes in the 40–430-cm^{-1} range and ≈17 modes in the 1430–1760-cm^{-1} range were observed, all of which have nearly equal intensity. Some of the most intense and ubiquitous Bchl$_a$ modes, such as the 332- and 730-cm^{-1} modes, are weak or not present. In addition, the spectra change significantly with small changes in excitation wavelength within a single absorption band. For instance, although at 25 K both 872 and 896 nm are resonant with the P absorption, the modes seen in the 872-nm spectrum at 270, 277, 303, and 340 cm^{-1} are not seen in the 896-nm spectrum. The 896-nm spectrum in turn exhibits modes at 253 and 288 cm^{-1}, which are not seen with any other excitation wavelength. By contrast, in our spectra, the same set of modes are consistently observed as excitation is tuned within the B or P bands, and the relative intensity patterns are maintained as excitation is tuned through each resonance. Further, as noted above, the modes reported here are in good agreement with previous vibronically-resolved experimental studies of Bchl$_a$-containing systems. Finally, we find the intensity of Raman scattering when on resonance with P to be ≈10 times less than that for Raman scattering from B. Palaniappan et al. report that scattering from P is as much as 15 times *greater* than scattering from B. *Thus, there are many significant and fundamental differences between our Raman data on P and B and that of ref 42.*

There are several differences in the experimental conditions, apparatus, and procedures that may explain this disagreement. First, the spectra reported here were taken at 278 K on samples of Q_A-containing, R-26 RCs flowing to ensure that photochemical products do not build up in the illuminated volume. The spectra taken by Palaniappan et al. were of stationary samples of chemically reduced (presumably Q_A-containing), wild-type (carotenoid-containing) RCs frozen at 201 and 25 K, conditions which could lead to photophysical or photochemical alteration. For example, Boxer et al. demonstrated that prolonged irradiation at 77 K leads to an increase in fluorescence, a change in sign of the fluorescence electric field effect, and a substantial decline in the quantum yield for charge separation between P and Q_A.[60] There effects were most pronounced in poly(vinyl alcohol) films but were also observed in frozen glasses. In addition, Small and co-workers recently reported accumulation of a modified form of the special pair during prolonged irradiation.[61] A second experimental difference is that the data presented here were acquired using the shifted excitation difference technique, while Palaniappan et al. mostly presented data acquired by direct detection followed by flat-field correction and subtraction of the fluorescence background. All of the strong features reported here in the shifted excitation spectra of B and P have also been observed using direct detection. However, longer exposure times are necessary to achieve satisfactory signal-to-noise, and in the presence of a fluorescence background 2–3 orders of magnitude more intense than the Raman scattering, extreme care is required in the flat-field correction and background subtraction steps to avoid artifacts. A third experimental difference is that the current work employed a front-illuminated CCD detector while Palaniappan et al. used a thinned back-illuminated detector. The quantum efficiency of the front-illuminated detector is approximately 2 times lower in the spectral range studied here. However, since all of our spectra were corrected for the variation in detector quantum efficiency, any differences in detection efficiency over the detection wavelength range should be canceled out. The front-illuminated CCD was selected for these experiments because we found that thinned back-illuminated detectors can have larger fluctuations in pixel-to-pixel sensitivity that are difficult to correct for when there is an intense fluorescence background.

Excited-State Dynamics of B and P. In addition to determining ground-state vibrational frequencies of B and P, information about excited-state dynamics can be obtained from resonance Raman spectra and Raman scattering intensities. The finding that the Raman cross sections are ≈10 times larger on resonance with B than with P could indicate that the excited-state dynamics are very different for the two chromophores. To examine the origin of the intensity difference between the B and P Raman cross sections, it is useful to consider the molecular parameters that control Raman intensities. A simple molecular model consists of a ground and an excited electronic state each having a potential energy surface consisting of independent harmonic oscillators. Each harmonic oscillator is characterized by a frequency, ω, and a displacement, Δ, where Δ is the shift in dimensionless normal coordinates between the equilibrium positions of the ground and excited electronic states. The Raman scattering intensity depends on the time-dependent overlap integral between the final vibrational state in the ground electronic state and a replica of the initial vibrational state that is evolving on the excited electronic state potential surface. This time-dependent overlap is determined by the Δ's and ω's for each mode, and the Fourier transform of the product of the function and a time-dependent damping function yields the Raman excitation profile.[45,46]

Part of the difference in Raman intensities between B and P may be due to large displacements in a number of modes in the excited state of P, causing a rapid damping of the time-dependent overlap and decreasing the Raman cross sections. On the other hand, B is likely to undergo only modest ground-to-excited state structural changes, like the Chl$_a$ monomer, where a total S ($S_{tot} = \sum_i \Delta_i^2/2$) of 0.8 was measured.[62] Hole-burning experiments on P[11,13] suggest a much larger total S of about 3.5. The two- or three-mode models used to model the hole burning can now be improved based on our demonstration that at least 14 modes are coupled to the electronic excitation of P. Multimode damping effects, in which a large displacement in one or more modes damps the Raman cross sections in all the modes, have been observed in other systems with large vibrational displacements.[63,64] In some cases, multimode damping effects result from displacements in modes that cannot be directly observed in the Raman spectrum, either because the vibrational frequency is too low or because the vibrational line width is so large that the Raman peak is buried in the Rayleigh or fluorescence background. Such unobserved modes act to increase the effective pure dephasing rate (vide infra), and so they are manifest in the magnitude of the phenomenological homogeneous damping function that is required to model the absolute Raman scattering intensities.

Resonance Raman scattering strength is also sensitive to electronic state dynamics through the damping function that multiplies the time-dependent overlap integral. A fast electronic dephasing time, T_2, will lead to smaller Raman cross sections. For room temperature condensed-phase systems, T_2 may have lifetime (T_1) and pure dephasing (T_2^*) contributions. The excited-state lifetimes of B and P have been studied. The lifetime of B* is controlled by the time for B*-to-P energy transfer. Though still an area of active study, it appears that this time is on the order of 100 fs,[25,65,66] while the lifetime of P* is about 3 ps.[20-25] Thus, the simplest analysis, in which the relative Raman scattering strengths of P and B are determined by electronic state dynamics, which in turn are controlled solely by T_1 processes, leads to the prediction that the resonance Raman cross sections of B will be smaller than those of P, while the observed cross sections of B are actually ≈10 times *larger* than those of P.

There are several other possibilities for explaining the different scattering strengths of B and P. Pure dephasing processes could contribute strongly to the room temperature T_2 in RCs, and the pure dephasing rates of B and P could be different depending upon each chromophore's environment and the interactions of its electronic states with the environment. Alternatively, rapid population dynamics (T_1 processes) other than the primary electron- or energy-transfer steps may contribute to the dephasing. For example, rapid vibrational relaxation in the excited electronic state of P could result in a fast effective T_1 for any vibronic transition. Such an explanation would, however, need to be reconciled with the interpretation that the oscillations observed by Vos et al. are due to vibrational coherence in the excited

electronic state.[24,33] Another possibility is that the electronic state structure of P is more complicated than has been implicitly assumed in the present discussion. There could be several nearly degenerate excited states of P, one of which might be a charge-transfer state.[19,67] In this case the dynamics associated with coupling between these states might affect the Raman cross sections of P.

In future work, the frequencies and coupling strengths derived from the resonance Raman intensity analysis of the B and P data will be used to produce a quantitative model for their excited-state nuclear and electronic dynamics. This will provide much needed multimode vibronic information to further interpret the results of low-temperature hole-burning experiments,[11,13] Stark effect studies,[16,17] and direct transient absorption and emission studies.[25,33] Such a unified view of the spectroscopy of reaction centers should provide insight into the excited-state nuclear dynamics and relaxation of the special pair and the primary electron-transfer reaction.

Acknowledgment. This work was funded in part by Grant CHE 91-20254 from the National Science Foundation to R.A.M. A.P.S. is supported by a National Institutes of Health Postdoctoral Fellowship (GM 14298). S.G.B. thanks the National Science Foundation Biophysics Program for its support.

References and Notes

(1) Abbreviations: special pair, P; accessory bacteriochlorophylls, B; reaction center, RC; Q_A, A-side quinone; bacteriochlorophyll$_a$, Bchl$_a$; Fourier transform, FT; Chl$_a$, chlorophyll$_a$.
(2) Kirmaier, C.; Holten, D. *Photosynth. Res.* **1987**, *13*, 225.
(3) Feher, G. *Annu. Rev. Biochem.* **1989**, *58*, 607.
(4) Friesner, R. A.; Won, Y. *Biochem. Biophys. Acta* **1989**, *977*, 99.
(5) Boxer, S. G.; Goldstein, R. A.; Lockhart, D. J.; Middendorf, T. R.; Takiff, L. *J. Phys. Chem.* **1989**, *93*, 8280.
(6) Verméglio, A.; Breton, J.; Paillotin, G.; Cogdell, R. J. *Biochim. Biophys. Acta* **1978**, *501*, 514.
(7) Rosenbach-Belkin, V.; Fisher, J. R. E.; Scherz, A. *J. Am. Chem. Soc.* **1991**, *113*, 676.
(8) Steffen, M. A.; Lao, K.; Boxer, S. G. *Science* **1994**, *264*, 810.
(9) Meech, S. R.; Hoff, A. F.; Wiersma, D. A. *Chem. Phys. Lett.* **1985**, *121*, 287.
(10) Boxer, S. G.; Lockhart, D. J.; Middendorf, T. R. *Chem. Phys. Lett.* **1986**, *123*, 476.
(11) Middendorf, T.; Mazzola, L.; Gaul, D.; Schenck, C.; Boxer, S. *J. Phys. Chem.* **1991**, *95*, 10142.
(12) Hayes, J. M.; Small, G. J. *J. Phys. Chem.* **1986**, *90*, 4928.
(13) Johnson, S. G.; Tang, D.; Jankowiak, R.; Hayes, J. M.; Small, G. J.; Tiede, D. M. *J. Phys. Chem.* **1989**, *93*, 5953.
(14) Reddy, N. R. S.; Small, G. J.; Seibert, M.; Picorel, R. *Chem. Phys. Lett.* **1991**, *181*, 391.
(15) Lockhart, D. J.; Boxer, S. G. *Biochemistry* **1987**, *26*, 664.
(16) Lösche, M.; Feher, G.; Okamura, M. Y. *Proc. Natl. Acad. Sci. U.S.A.* **1987**, *84*, 7537.
(17) Lockhart, D. J.; Boxer, S. G. *Proc. Natl. Acad. Sci. U.S.A.* **1988**, *85*, 107.
(18) Middendorf, T. R.; Mazzola, L. T.; Lao, K.; Steffen, M. A.; Boxer, S. G. *Biochim. Biophys. Acta* **1993**, *1143*, 223.
(19) Won, Y.; Friesner, R. A. *Proc. Natl. Acad. Sci. U.S.A.* **1987**, *84*, 5511.
(20) Woodbury, N. W.; Becker, M.; Middendorf, D.; Parson, W. W. *Biochemistry* **1985**, *24*, 7516.
(21) Martin, J.-L.; Breton, J.; Hoff, A. J.; Migus, A.; Antonetti, A. *Proc. Natl. Acad. Sci. U.S.A.* **1986**, *83*, 957.
(22) Kirmaier, C.; Holten, D. *Proc. Natl. Acad. Sci. U.S.A.* **1990**, *87*, 3552.
(23) Holzapfel, W.; Finkele, U.; Kaiser, W.; Oesterhelt, D.; Scheer, H.; Stilz, H. U.; Zinth, W. *Proc. Natl. Acad. Sci. U.S.A.* **1990**, *87*, 5168.
(24) Vos, M. H.; Lambry, J.-C.; Robles, S. J.; Youvan, D. C.; Breton, J.; Martin, J.-L. *Proc. Natl. Acad. Sci. U.S.A.* **1991**, *88*, 8885.
(25) Du, M.; Rosenthal, S. J.; Xie, X.; DiMagno, T. J.; Schmidt, M.; Hanson, D. K.; Schiffer, M.; Norris, J. R.; Fleming, G. R. *Proc. Natl. Acad. Sci. U.S.A.* **1992**, *89*, 8517.
(26) Myers, A. B.; Harris, R. A.; Mathies, R. A. *J. Chem. Phys.* **1983**, *79*, 603.
(27) Sue, J.; Mukamel, S. *J. Chem. Phys.* **1988**, *88*, 651.
(28) Loppnow, G. R.; Mathies, R. A. *Biophys. J.* **1988**, *54*, 35.
(29) Phillips, D. L.; Myers, A. B. *J. Chem. Phys.* **1991**, *95*, 226.
(30) Morikis, D.; Li, P.; Bangcharoenpaurpong, O.; Sage, J. T.; Champion, P. T. *J. Phys. Chem.* **1991**, *95*, 3391.
(31) Shreve, A. P.; Cherepy, N. J.; Franzen, S.; Boxer, S. G.; Mathies, R. A. *Proc. Natl. Acad. Sci. U.S.A.* **1991**, *88*, 11207.
(32) Shreve, A. P.; Cherepy, N. J.; Mathies, R. A. *Appl. Spectrosc.* **1992**, *46*, 707.
(33) Vos, M. H.; Rappaport, F.; Lambry, J.-C.; Breton, J.; Martin, J.-L. *Nature* **1993**, *363*, 320.
(34) Schenck, C. C.; Blankenship, R. E.; Parson, W. W. *Biochim. Biophys. Acta* **1982**, *680*, 44.
(35) Okamura, M.; Isaacson, R.; Feher, G. *Proc. Natl. Acad. Sci. U.S.A.* **1975**, *72*, 3491.
(36) Mathies, R.; Yu, N.-T. *J. Raman Spectrosc.* **1978**, *7*, 349.
(37) Mathies, R.; Oseroff, A. R.; Stryer, L. *Proc. Natl. Acad. Sci. U.S.A.* **1976**, *73*, 1.
(38) The path length traveled by the emission between the sample and the detector is approximately 4 m. For this path length, water vapor absorption results in easily discernible structure in the 925–960-nm region superimposed upon the broad fluorescence emission from the RCs. Experimentally, as much as 5% of the dispersed light, if resonant with a rovibrational water transition, is absorbed, in agreement with literature values for water absorption cross sections of $\approx 10^{-21}$ cm^2/molecule in this region.[39,40] In comparison, the underlying Raman features are $\approx$0.1% of the fluorescence background. When two spectra are subtracted using the shifted excitation difference technique, the relatively large water absorptions produce noise on the scale of the Raman features, apparently because of small fluctuations in intensities of the water lines from spectrum to spectrum. Purging the spectrograph with N_2 eliminates this interference.
(39) Chevillard, J.-P.; Mandin, J.-Y.; Flaud, J.-M.; Camy-Peyret, C. *Can. J. Phys.* **1989**, *67*, 1065.
(40) Chu, Z.; Wilkerson, T. D.; Singh, U. N. *Appl. Opt.* **1993**, *32*, 992.
(41) Zankel, K.; Reed, D.; Clayton, R. *Proc. Natl. Acad. Sci. U.S.A.* **1968**, *61*, 1243.
(42) Palaniappan, V.; Aldema, M. A.; Frank, H. A.; Bocian, D. F. *Biochemistry* **1992**, *31*, 11050.
(43) Warshel, A. *Annu. Rev. Biophys. Bioeng.* **1977**, *6*, 273.
(44) Champion, P. M.; Albrecht, A. C. *Annu. Rev. Phys. Chem.* **1982**, *33*, 353.
(45) Heller, E. J.; Sundberg, R. L.; Tannor, D. *J. Phys. Chem.* **1982**, *86*, 1822.
(46) Myers, A. B.; Mathies, R. A. In *Biological Applications of Raman Spectrometry*; Spiro, T. G., Ed.; John Wiley: New York, 1987; p 1; Vol. 2.
(47) Warshel, A. *Proc. Natl. Acad. Sci. U.S.A.* **1980**, *77*, 3105.
(48) Mattioli, T. A.; Hoffmann, A.; Lutz, M.; Schrader, B. *C.R. Acad. Sci. Paris, Ser. III* **1990**, *310*, 441.
(49) Noguchi, T.; Furukawa, Y.; Tasumi, M. *Spectrochim. Acta* **1991**, *47A*, 1431.
(50) Lutz, M.; Mäntele, W. In *Chlorophylls*; Scheer, H., Ed.; CRC Press: Boca Raton, FL, 1991; p 855.
(51) Robert, B. *Biochim. Biophys. Acta* **1990**, *1017*, 99.
(52) Johnson, C. K.; Rubinovitz, R. *Spectrochim. Acta* **1991**, *47A*, 1413.
(53) Mattioli, T. A.; Hoffmann, A.; Sockalingum, D. G.; Schrader, B.; Robert, B.; Lutz, M. *Spectrochim. Acta* **1993**, *49A*, 785.
(54) Mattioli, T. A.; Hoffmann, A.; Robert, B.; Schrader, B.; Lutz, M. *Biochemistry* **1991**, *30*, 4648.
(55) Calculations of the Raman cross sections of B show that while all cross sections decrease as excitation is tuned off resonance, the cross sections of the high-frequency modes decrease less rapidly than those of the low-frequency modes. This suggests that the 1064-nm excitation FT Raman spectra would show relatively strong high-frequency scattering as compared to the resonantly excited spectra.
(56) Donohoe, R. J.; Dyer, R. B.; Swanson, B. I.; Violette, C. A.; Frank, H. A.; Bocian, D. F. *J. Am. Chem. Soc.* **1990**, *112*, 6716.
(57) Renge, I.; Mauring, K.; Avarmaa, R. *J. Lumin.* **1987**, *37*, 207.
(58) van der Laan, H.; Smorenburg, H. E.; Schmidt, T.; Völker, S. *J. Opt. Soc. Am. B* **1992**, *9*, 931.
(59) Small, G. J.; Hayes, J. M.; Silbey, R. J. *J. Phys. Chem.* **1992**, *96*, 7499.
(60) Boxer, S. G.; Franzen, S.; Lao, K.; Lockhart, D. J.; Stanley, R.; Steffen, M.; Stocker, J. W. In *The Photosynthetic Bacterial Reaction Center II: Structure, Spectroscopy, and Dynamics*; Breton, J., Vérmeglio, A., Eds.; Plenum Press: New York, 1992; p 271.
(61) Raja, N.; Reddy, S.; Kolaczkowski, S. V.; Small, G. J. *Science* **1993**, *260*, 68.
(62) Gillie, J. K.; Small, G. J.; Golbeck, J. H. *J. Phys. Chem.* **1989**, *93*, 1620.
(63) Reid, P. J.; Shreve, A. P.; Mathies, R. A. *J. Phys. Chem.* **1993**, *97*, 12691.
(64) Lawless, M. K.; Mathies, R. A. *J. Chem. Phys.* **1994**, *100*, 2492.
(65) Breton, J.; Martin, J.-L.; Migus, A.; Antonetti, A.; Orszag, A. *Proc. Natl. Acad. Sci. U.S.A.* **1986**, *83*, 5121.
(66) Breton, J.; Martin, J.-L.; Fleming, G. R.; Lambry, J.-C. *Biochemistry* **1988**, *27*, 8276.
(67) Lathrop, E. J. P.; Friesner, R. A. In *The Photosynthetic Reaction Center II: Structure, Spectroscopy, and Dynamics*; Breton, J., Verméglio, A., Eds.; Plenum Press: New York, 1992; p 183.